World Conference on Timber Engineering
Oslo 2023

SEISMIC PERFORMANCE OF CLT SHEAR WALL INFILLED HYBRID STEEL MOMENT FRAME WITH CONCEALED STEEL PLATE AND DRIFT PINS CONNECTIONS

Hiroshi Isoda[1], Richard Yip Je Too[2], Kazumi Kanazawa[3]

ABSTRACT: In Japan, the recent introduction of Cross Laminated Timber (CLT) started gaining attention because of its ability to perform under seismic activities. The increasing of utilization of timber in mid-rise buildings became possible followed by the change in height limit of fire-proofed timber buildings (e.g., Steel-CLT hybridization) in the Building Standard Law. However, the design method of such hybrid structures in Japan has yet to be generalized and it has become an obstacle for structural designers. In this paper, a series of models for hybrid steel moment frame (SMF) CLT shear walls structures are presented for the non-linear incremental displacement analysis. The model was verified by the experiment results and can potentially serve as an appropriate method to design future CLT-Steel hybrid structures.

KEYWORDS: Cross Laminated Timber, Hybrid Structures, Lateral Performance, Cyclic Tests

1. INTRODUCTION

Hybrid systems require an application of 2 or more materials and enable the benefits of each material to be applied to seismic force resisting systems. For instance, in timber and steel hybridization, the ductility of steel provides significant post-yield deflection capability, allowing the structure to dissipate seismic energy during earthquakes. On the other hand, the timber infill can increase the stiffness of the system, which can reduce the fundamental period and drift values in seismic vulnerability. [1]

Recently, many researchers are beginning to focus on research topics regarding steel-timber hybrid buildings. In Canada, research on steel-timber hybrid system was conducted [2]. The proposed system consists of a steel beams with wooden shear wall infills connected to the studs via nails. In China, a hybrid system consisting a steel frame with wooden shear wall infill was proposed, in which nails were also used to connect the wooden shear walls [3]. From the results, it was observed that the timber infill could contribute to the increase of stiffness and strength of the structure significantly. Nonetheless, ultimate failures like panel tear out and bending of nails were observed. The failures show that the stiffness and strength of the connection is inadequate, indicating that the system could resist more load if properly designed with stronger connection, as well as with stronger infills.

To overcome such problems, a new steel-timber hybrid system is proposed in this paper. It utilizes concealed plate with drift pin (DP) connections as the wall-to-frame connection and cross laminated timber (CLT) as the infill wall for better seismic performance. The advantages of using DP connectors is that, it can have high ductility like nails and screws, while also maintaining its high rigidity. In Japan, the research on steel-timber hybrid system utilizing concealed steel plate with DP connection was initially conducted by Fukumoto et. al. [4]. However, the system consists of steel tie bars as well, which are exposed, and fire safety would become an issue. Because of this, newly developed wall-to-frame connection was proposed that consists of only DP connections with concealed steel plate inserted into the pre-opened slit in the CLT panel.

In 2018, Kanazawa et. al. [5] reported the results on this type of hybrid system for the first time. In 2019, 4 new types of specimens were additionally introduced, of which the results have not been reported anywhere else. On top of that, in Japan, the standard seismic design methodology for such hybrid system has not been generalized. Therefore, this paper will compare and discuss the results of all 2018 and 2019 specimens and also to propose an analysis model that can trace the cyclic behaviour of the system. The model could serve as a fundamental design methodology with the aim to accelerate the promotion of such hybrid system. It should be noted that the presented contents in this paper are a part of the journal paper accepted for publication, written by Richard et al [6]. For more information, please refer to the paper listed in the reference.

2. DESCRIPTION OF TEST SPECIMENS

Figure 1 and 2. shows the naming method of the specimens and the detailed figure of the standard hybrid specimen FM-S60-32, respectively. Figure 3 and 4. show the specimen overview of tests conducted in 2918 and 2019, respectively. It should be noted that the CLT-steel hybrid frame experiment was conducted at 1/2 scale. The size of the specimens is 3600mm and 2000mm between

[1] Hiroshi Isoda, Research Institute for Sustainable Humanosphere, Kyoto university, Japan, hisoda@rish.kyoto-u.ac.jp
[2] Richard Yip Je Too, Research Institute for Sustainable Humanosphere, Kyoto university, Japan,
[3] Kazumi Kanazawa, Research and Development Institute, Takenaka Corp., Japan. (former graduate student at Kyoto University)

https://doi.org/10.52202/069179-0455

the center of steel columns and steel beams, respectively. The steel column is SN490B graded with size of RH-300x300x10x15 for all specimens. Column and beam connections are rigidly welded and reinforcing ribs were appropriately placed in

each specimen. The CLT panel used in the experiment is made of Japanese Cedar, which is 1531mm in height (1631mm for FS-S60-32), 1100mm in width (1075mm for FM-S60-32-S) and 105mm in thickness. At the wall-to-frame connection, concealed steel plate and DP connections are applied. To further connect the concealed steel plate to the steel frame, several bolts were used. The length and the DPs were 105mm and 10mm, respectively. The thickness of the concealed steel plate was 6mm. Moreover, non-shrink mortar was also infilled in between the CLT panel and the frame, to increase fire safety as well as to cover the uneven surfaces of the steel beam for better distribution of the compression load from the CLT panel.

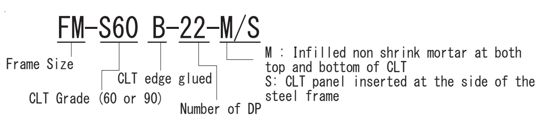

Figure 1: *Naming method of the specimens*

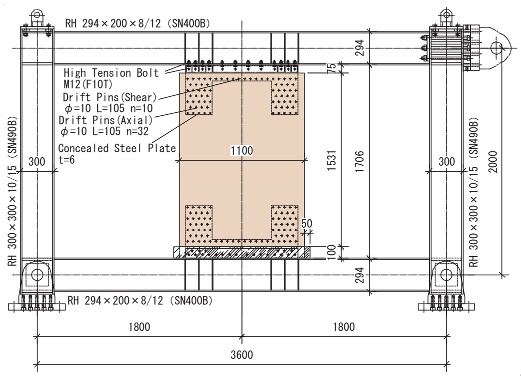

Figure 2: *Detailed figure of FM-S60-32*

In this paper, a total of 8 specimens, including 2 steel bare frame and 6 CLT-steel hybrid specimens with different configurations were prepared and investigated. The parameters of the hybrid specimens, including the descriptions are listed as follows:

1. Stiffness grading of CLT panel(S60 or S90): Specimen that consists of CLT infill with higher grading (S90) was introduced to investigate its effectiveness in the hybrid system, compared to the lower graded CLT (S60).

2. Edge gluing between the laminas in the CLT panel: To investigate the difference in the amount of contribution to the overall shear resistance due to the increased performance provided by the edge gluing in the CLT shear wall.

3. Positioning of CLT panel: To investigate the effectiveness of the shear force resisted by the infilled CLT shear wall when it is placed at the side of the steel frame.

4. Number of drift pins (22 or 32): To investigate the influence of the number of drift pins (32+10+32 or 22+14+22 configuration) on the lateral performance of the hybrid system.

5. Position of infill non-shrink mortar: To investigate the effect of a higher stiffness option due to the stronger compressive strut formed in the CLT shear wall.

6. Size of the steel beam (FS:RH-194x150x6x9 or FM:RH-294x200x8x12, both SN490N graded): To investigate the capability in energy dissipation which occurs through the yielding of the steel beam.

3. TESTING METHODS AND DATA ACQUISITION

Figure 5. illustrates the setup of the cyclic loading test and the measuring positions for data acquisition. The test specimen was pushed and pulled by two hydraulic

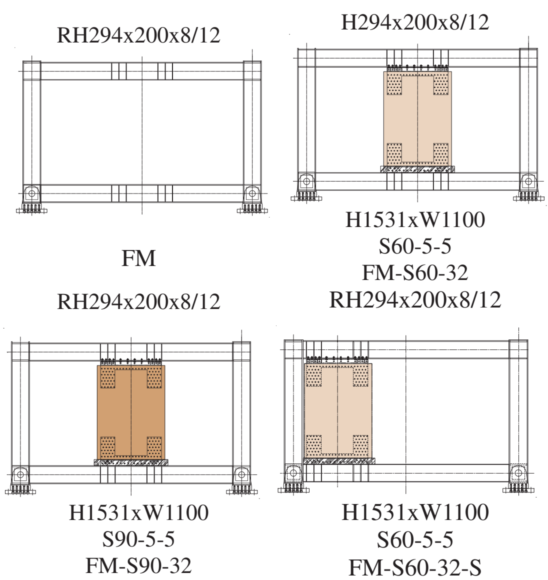

Figure 3: *Overview of stage 1 specimens*

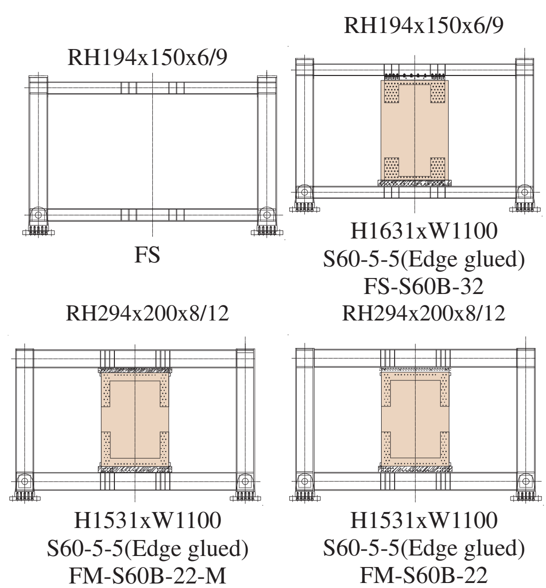

Figure 4: *Overview of stage 2 specimens*

https://doi.org/10.52202/069179-0455

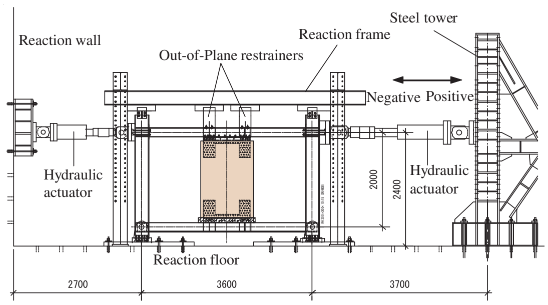

Figure 5: *Configuration of cyclic loading test*

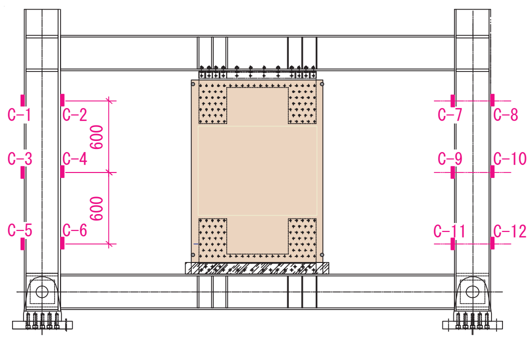

Figure 6: *Position of strain gauges on steel columns*

actuators from both sides of the frame. Out-of-plane restrainers were set above the top of the steel beam to prevent out of plane deformation. The steel frame was also fixed to the reaction floor.

The horizontal displacement δ was measured at the centre of top steel beam. The drift angle R is calculated by δ/H, where H is the distance between centre of the beams (=2000mm).

To evaluate the shear force in each of the steel frame and the CLT infill, the following equations were used. The shear force resisted by the steel frame (Qc) can be obtained by adding the shear forces in the left (Q_{CL}) and right (Q_{CR}) steel columns. The shear force in each steel column was determined using Equation (1).

$$Q_{CL}\ or\ Q_{CR} = \frac{M_{top} + M_{bottom}}{h} = \frac{(\varepsilon_{top} + \varepsilon_{bottom})EZ}{2h} \tag{1}$$

In Equation (1), M_{top} and M_{bottom} are the bending moments of the top part and bottom part of each steel column, ε_{top} and ε_{bottom} are the strain values recorded using strain gauges located at the top (C-1, C-2 and C-7, C-8) and bottom (C-5, C-6 and C-11, C-12) of the steel columns, respectively, shown in Figure 6. E is the elastic modulus of steel (2.05x10^5 N/mm^2), Z is the section modulus of the steel columns (1.35x10^6 mm^3), and h is the vertical distance between the strain gauges (1,200 mm).

In the CLT-Steel hybrid wall system, the total shear force (Q) was resisted by two components, the steel frame and the CLT shear wall. Therefore, from the load-sharing by the two components, Q_{CLT} can be acquired by using Equation (3).

$$Q_C = Q_{CL} + Q_{CR} \tag{2}$$

$$Q_{CLT} = Q - Qc \tag{3}$$

It should be noted that both stage 1 and 2 test specimens were subjected to different cyclic loading protocol of controlled angular displacement with cycles grouped in phases, as indicated in Figure 7. Even though the loading protocols were different, the obtained results for both stages were essentially the same. The first phase for 1/200 rad contains only 2 full reversed cycles for stage 2 specimens, while others contain 3 cycles. Finally, the loading will be terminated at final pushover at 1/10rad, where the specimens are expected to fail.

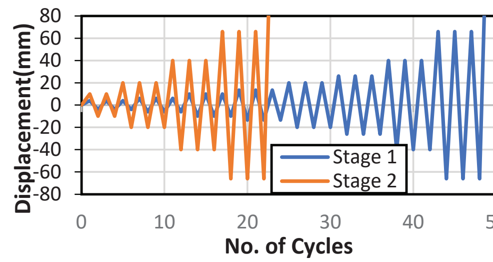

Figure 7: *Loading protocol*

4. RESULTS AND DISCUSSIONS.

4.1 Load-Displacement Properties

Figure 8. summarizes the load-displacement hysteresis curves of all specimens. From the figures, it can be observed that with the exception of FM-S60-32-S, the CLT-infilled specimens with FM beams experienced strength degradation at an angular deformation of around 1/50 to 1/30 rad due to the shear failure of the CLT infill. It can be said that the shear capacity of the CLT infill was fully utilized. As for FS-S60B-32, strength degradation did not occur because one of the two steel beams yielded and buckled markedly at 1/30 rad, which led to out-of-plane deformation of the CLT infill. All the specimens were tested successfully, per the loading schedule, except for specimen FM-S60-32-S, for which the test had to be terminated prematurely because of the large compression flange local buckling of the beam. Overall, almost no slip behaviour was observed among the hysteretic behaviour of the specimens with CLT infill, an outcome that was similar to the hysteretic behaviour of the steel frame specimens. This shows that the steel frame was dominant in terms of the behaviour of the hybrid system.

Table 1 summarizes the specimens' maximum capacity and initial stiffness. The table shows that the installation of the CLT panel significantly increased the maximum load capacity and initial stiffness of the steel bare frame. From Figure 8 and Table 1, the following principal conclusions can be drawn:

1. When comparing specimen FS-S60B-32 and FM Frame to FS frame, the results show that same amount of increase in maximum capacity and initial stiffness were obtained in both cases. Considering that there was no strength degradation occurred in FS-S60B-32, it indicates that by

https://doi.org/10.52202/069179-0455

infilling a CLT panel into a slender frame, the hybrid system is capable of increasing the stiffness while still maintaining the ductility.

2.When comparing FM framed hybrid specimens to FM frame, the results show that the reinforcement effect in maximum capacity and initial stiffness by the CLT infill is lower compared to FS-S60B-32. Although strength degradation occurred in FM framed hybrid specimens, the amount is not large overall, demonstrating that the lateral load was shared by both the steel frame and the infill, which worked closely together to resist lateral load.

4.2 Typical Failure Modes

In this section, the typical failure modes of the hybrid systems are presented. At 1/100rad, noticeable displacement at the DP connections was observed in specimens with fewer DP connectors. Due to the yielding of DP connectors, specimens FM-S60B-22 and FM-S60B-22-M were observed to undergo early failure at the wall-to-frame connection, of a type that involved compressive buckling at the concealed steel plate as shown in Figure 9(a). Between 1/50 and 1/30rad, all specimens except specimen FS-S60B-32 underwent shear failure along the grain of CLT's lamina, as shown in Figure 9(b). Because of the early yielding of DP connectors, specimens FM-S60B-22-M and FM-S60B-22 showed particularly significant failure in the CLT shear wall, which split in half vertically in the middle as shown in Figure 9(c). However, in the case of FM-S60B-22-M, the lateral load was maintained even after the splitting, as the mortar at top and bottom constrained the potential rocking motion of the split CLT, thus enabled each broken section to continue to resist lateral load individually.

At large deformations (1/50 rad~1/10 rad), the steel frame began to display yielding evidence, thereby demonstrating the capability to dissipate energy through plastic deformation. While yielding of the steel frame was observed in all specimens, it is noticeable that the DPs in specimens with 22+14+22 configurations underwent yield deformation before yielding of the steel frame; this proved the capability to dissipate energy at smaller deformations. After the experiments were concluded, almost all the specimens with infilled CLT shear walls were observed to have experienced the separation of a CLT panel from a concealed steel plate at one or more locations, as shown in Figure 9(d). This was because of the repetitive bending deformation of the DPs under a growing angular cyclic displacement.

4.3 Load Sharing Effect

As described above, in the CLT-steel hybrid system, the shear force is jointly resisted by the CLT panel and the columns of the steel frame. In order to evaluate the effectiveness of the hybrid system's lateral load resistance, the percentage of shear force resisted by each of the subsystems was calculated for all specimens using the values of Eqs. (2) and (3); the results are shown in Figure 10. The percentage of utilized CLT shear capacity calculated using Eq. (4) is also shown,

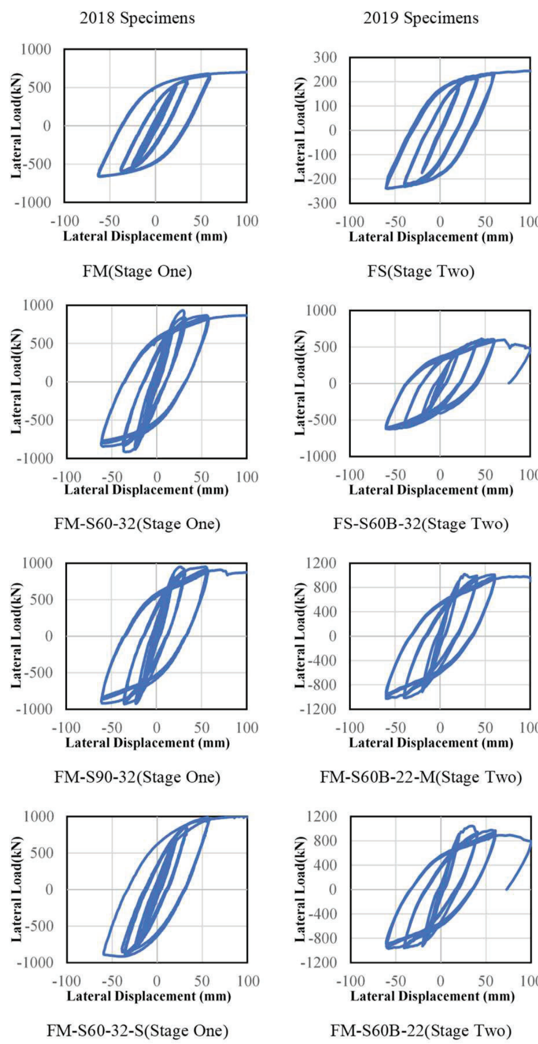

Figure 8: *Load-Displacement Skeleton Curves*

Table 1: Maximum capacity and initial stiffness

Specimen Name	Maximum capacity(kN)		Initial stiffness (kN/mm)	
	P_{max}	Compare to FS* or FM frame	K	Compare to FS* or FM frame
FS	247.5	-	8.5	-
FS-S60B-32	611.5	2.5*	25.6	3.0*
FM	791.3	2.9*	24.32	3.2*
FM-S60-32	931.7	1.2	46.08	1.9
FM-S90-32	931.7	1.2	51.88	2.1
FM-S60-32-S	1003.4	1.3	37.11	1.5
FM-S60B-22-M	1015	1.3	55.74	2.3
FM-S60B-22	1045	1.3	51.56	2.1

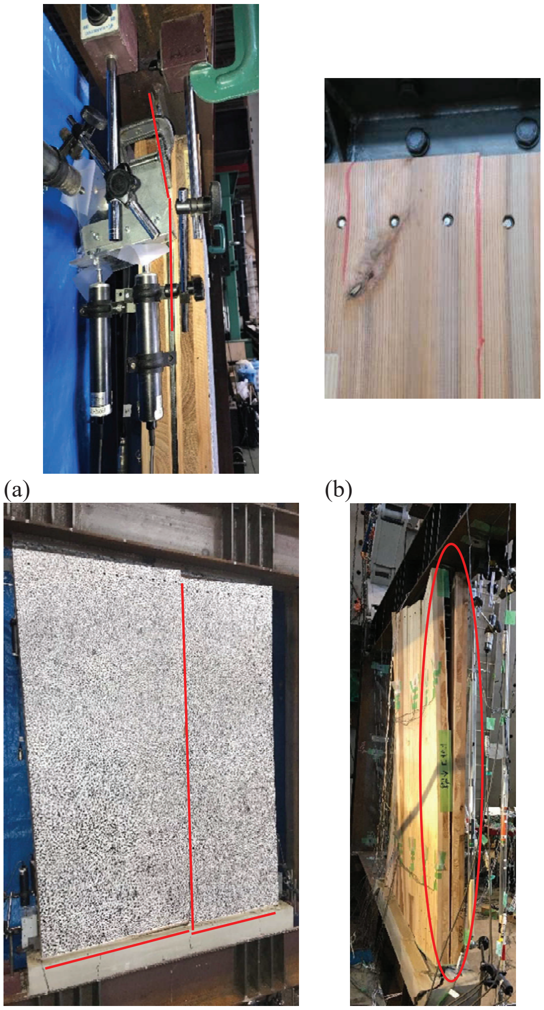

(a) (b) (c) (d)

Figure 9: *Failure mechanisms*

$$Q_{CLT(\%)} = \frac{Q_{CLT}}{\min\{Q_s, Q_m\}} \times 100 \tag{4}$$

where, Q_{CLT} is the shear force resisted by the CLT during the test, and $\min\{Q_s, Q_m\}$ is the calculated CLT shear strength (268.9kN for S60 and 311.9kN for S90).

In the case of FS-S60B-32, at the initial cyclic deformation of 1/200 rad, 50% of the shear capacity of CLT was utilized. As the deformation progressed, the shear capacity was utilized up to 127% at peak. In terms of the sharing of resistance between the panel and the frame, the CLT infill resisted more than half of the shear force until almost the end of the experiment without any strength degradation. That was because, as compared with tests based on the FM frame, this specimen used the more slender FS beams. Because of that, this specimen was observed to experience significant torsional buckling at 1/30 rad, which led to the out-of-plane deformation of CLT.

For the other five specimens, a different result was observed. The shear capacity of the CLT was taken

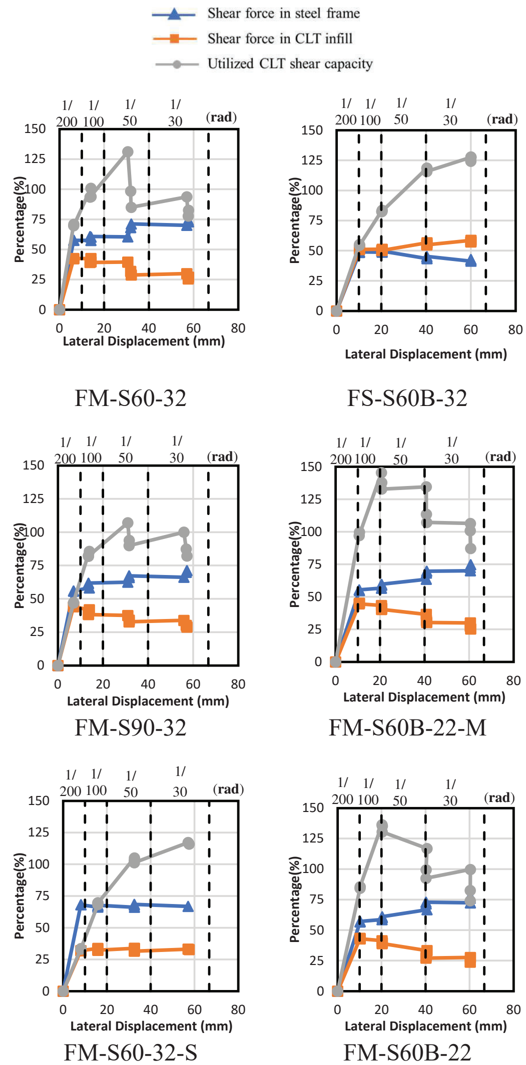

Figure 10: *Load sharing effect between steel frame and CLT infill*

advantage of at a comparatively smaller deformation, especially those specimens that had a 22+14+22 DP configuration. This is because of the early yielding of the DP connectors, which caused the CLT to deform more freely, a fact which also resulted in early shear failure of the CLT. Overall, the shear capacity of the CLT was utilized to beyond 100% (107~145%) in every specimen, proving that the utilization of the shear capacity of CLT infill was maximized. As for the sharing of the load, the steel frame resisted more than 50% of the shear force throughout the experiment because of the more robust beams, which were more capable of transferring the lateral loads to the steel columns. As observed in the discussion of failure mechanisms, the CLT could still resist some shear force even after shear failure. Due to the accumulation of damage, the percentage of force resisted by the CLT infill nonetheless decreased gradually, as shown in Figure 10.

https://doi.org/10.52202/069179-0455

5. NUMERICAL ANALYSIS

5.1 Analysis Model

A hysteresis model that can accurately reflect the hybrid

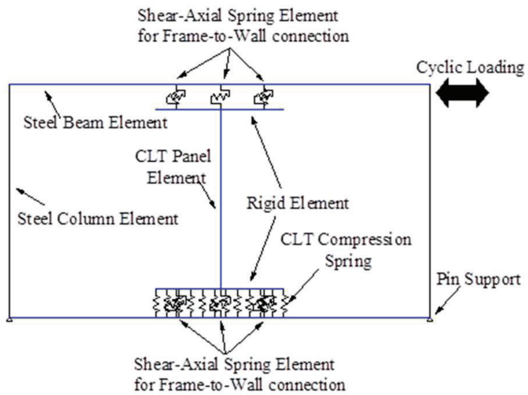

Figure 11: *Analysis model for specimen FM-S60-32*

system's behaviour was developed using a commercial

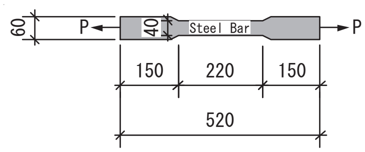

(a) Steel bar tensile test

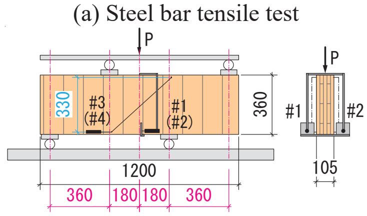

(b) CLT shear test

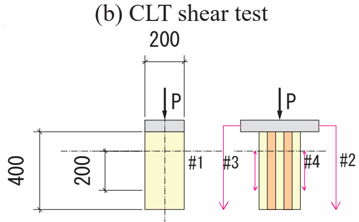

(c) CLT compression test

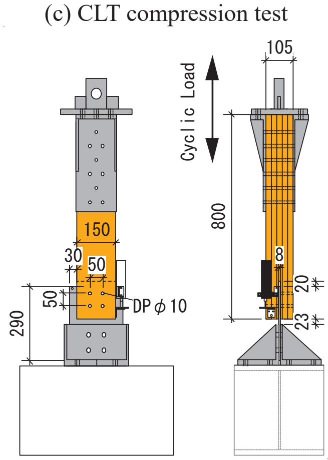

(d) Drift pin cyclic test

Figure 12: *Overview of elemental tests*

software, SNAP V7.0 [7]. The analysis model for specimen FM-S60-32 is shown in Figure 11, as an example for the overall explanation. Figure 12 provides an overview of a series of elemental tests conducted to help define the parameters of each component in the model.

Firstly, the hysteretic response of the steel frame was reproduced and confirmed through validation with the test results of the steel bare frame specimens. The bare frame model is basically the same as the example shown in Figure 11, minus the CLT infill elements. The hysteretic

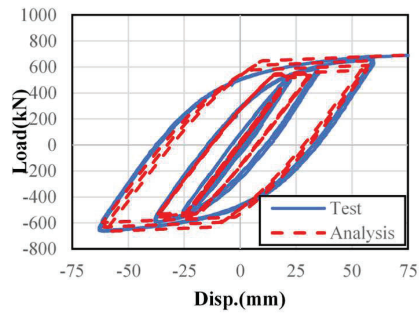

Figure 13: *Comparison between the test and numerical results of FM steel bare frame*

response of the steel frame was reproduced using the proposed modified Ramberg-Osgood model [8]. The parameter values used to define the steel frame model were obtained from the steel bar tensile test, illustrated in Figure 10(a). A good agreement between the experimental and analytical results was obtained, as shown in Figure 13.

As for the CLT infill, it was modelled as an I shape with a vertical beam element in the middle and horizontal beam elements on the top and the bottom. During the experiments, strength degradation occurred due to the shear failure of the CLT infill. To reproduce such behaviour, the vertical beam element is defined as non-linear with model that allows strength degradation. The shear properties of the CLT infill were obtained from the CLT shear elemental test, illustrated in Figure 12(b). On the other hand, the horizontal beam elements were defined as rigid to allow effective load transfer between the CLT and steel frame through the DP connections in the numerical model. The contact surface between the CLT infill and the non-shrink mortar was modelled using a series of spring elements placed 100mm apart. Each of the bearing spring was adjusted to only resist compression and modelled as an elastic-plastic element, of which the parameter input was obtained from the CLT compression test illustrated in Figure 12(c). However, the bearing springs at the ends were considered to only have half the stiffness and yield strength, as each of the bearing springs is assumed to bear the compression load by a certain area.

Finally, the wall-to-frame connections (drift pin connections) was modelled using a series of axial-shear spring elements, which can resist both axial tensile and compression, as well as shear forces. The hysteretic behaviour of the connection was represented using the

https://doi.org/10.52202/069179-0455

modified NCL model, proposed by Matsunaga et al. [9]. As illustrated in Figure 12(d), the drift pin cyclic test was conducted to obtain the load-deformation relationships for

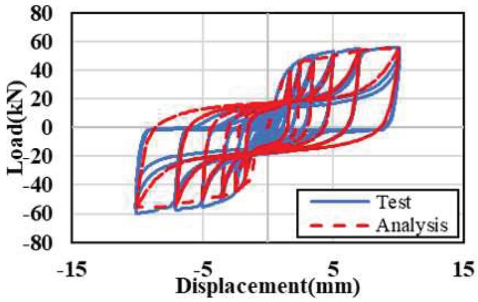

Figure 14: *Comparison between the drift pin cyclic test and calibrated numerical result*

the frame-to-wall connection. The elemental test results were then used for calibration to obtain the parameters of the modified NCL model. It can be seen from the comparison of the analysis result and the test result in Figure 14, the calibration went well as the model is capable of reproducing the slip and pinching behaviour of the DP connection under cyclic loading.

5.2 Modelling Results

The analysis model was subjected to the same loading protocol as the structural experiments. The predicted hysteresis loops, load sharing effect and cumulative energy dissipation (obtained by calculating the area under the hysteresis loops) of the hybrid system are shown in Figure 15, 16 and 17. Since the modelling results are similar for all specimens, only the results for FM-S60-32 specimen are shown.

From Figure 15, it can be observed that the plotting of the yielding of steel beam, shear failure of CLT and yielding of DP from the test and analysis results are in good agreements. Generally, the numerical results were able to reproduce the hysteretic behaviour of the hybrid system; a behaviour that is governed by the steel frame.

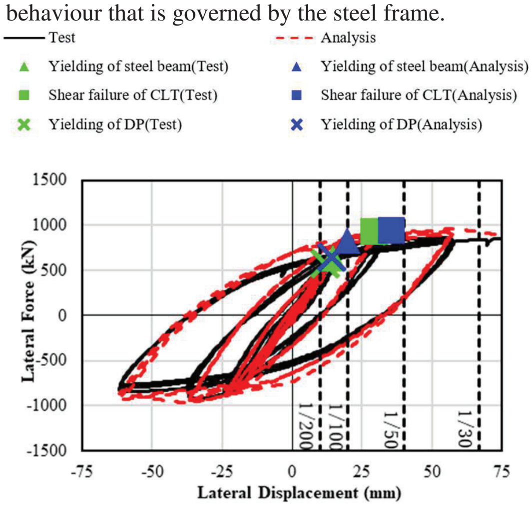

Figure 15: *Predicted hysteresis loops*

From Figure 16 and Figure 17, it can be seen that the model predictions were capable of capturing the trend of the load sharing effect between the two subsystems (steel frame and CLT) and also the cumulative energy dissipation at all test cycles.

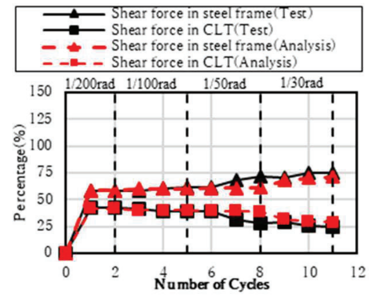

Figure 16: *Load sharing effect (Test vs. Analysis)*

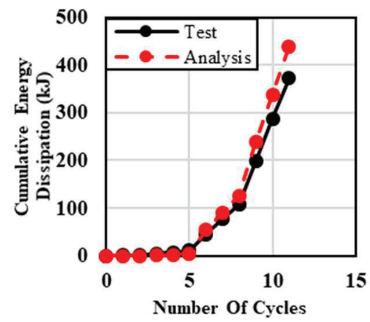

Figure 17: *Cumulative Energy Dissipation (Test vs. Analysis)*

6. CONCLUSIONS

This paper reports the experimentally observed and numerically simulated performance of a CLT-steel hybrid system using concealed steel plates and drift pins as wall-to-frame connections in different configurations. The load-displacement properties, failure mechanisms, equivalent viscous damping factors, and shear force sharing effect between the timber and steel subsystems were observed and discussed.

From the load-displacement properties, it was observed that significant increases in initial stiffness and maximum capacity for the bare steel frame could be obtained by infilling a CLT shear wall. At large deformations, most of the specimens were seen having an ultimate failure at the wall-to-frame connection, for example, shear failure of the bolted connection, buckling failure of the moment-bearing concealed steel plate, and detachment of the CLT panels from the moment-bearing concealed steel plate. As for the sharing of shear force between the CLT panel and the steel frame, the results showed that both of these components worked closely together to resist the lateral load. In general, the burden of resistance increased for the steel frame once damage developed in the CLT infill. Also, when the steel beam size was larger than the two under test (M frames as opposed to S frames), the steel columns could resist most of the lateral load due to the more effective transfer of load from the beam.

https://doi.org/10.52202/069179-0455

After the structural experiments were concluded, a non-linear finite element model was developed using SNAP V7.0 for the purpose of simulating the experimental results and as a basis for making further predictions. Three sub-models were made of the frame, the CLT panels, and the frame-panel connections, respectively, and combined to reproduce the experimental results accurately. The results of the numerical model did reliably agree with the experimental results. Such validation of the numerical model by the experimental results means that the model is a candidate to serve as a tool for designing such wood-steel hybrid structures, intended for applications as lateral load resisting systems for medium- to high-rise buildings in Japan. In addition, for further studies, the numerical model may be used to conduct seismic analyses to determine appropriate R-factors, which are required when designing such structures.

ACKNOWLEDGEMENT

This research was supported by the Forestry Agency under Ministry of Agriculture, Forestry and Fisheries. (Project Title: Development of seismic wall construction technology for wood-based materials such as CLT, 2018)

REFERENCES

[1] Tesfamariam, S., S. Stiemer, C. Dickof, and M. Bezabeh. (2014): Seismic Vulnerability Assessment of Hybrid Steel-Timber Structure: Steel Moment-Resisting Frames with CLT Infill, Journal of Earthquake Engineering, 18:6, 929-944

[2] Stiemer, S. F., S. Tesfamariam, E. Karacabeyli, and M. Propovski. 2012. "Development of steel-wood hybrid systems for buildings under dynamic loads." In *Proc., 7th Int. Specialty Conference on Behaviour of Steel Structures in Seismic Areas (STESSA).* Abingdon, England: CRC Press.

[3] Li, Z., X. Wang, M. He, W. Dong, and H. Dong. 2019. "Seismic performance of timber-steel hybrid structures. I: Subassembly testing and numerical modeling." *J. Struct. Eng.,* 145 (10), 04019113. https://doi.org/10.1061/(ASCE)ST.1943-541X.0002395.

[4] Fukumoto, K., Kouda, M., Kubo, K., Usami, T., Kitamori, A., Miyauchi, Y. and Isoda, H. "Experimental Study on CLT Seismic Panel Infilled within Steel Frame, Buildings, Journal of Structural and Construction Engineering" (Transaction of AIJ), Vol.86, No.787, pp.1345-1356, 2021.9 (in Japanese) https://doi.org/10.3130/ajis.86.1345

[5] Kanazawa, K., Isoda, H., Kitamori, A., Usami, T. and Araki, Y. "Structural Performance of Composite Structure with CLT Wall Infilled In Steel Frames Using Drift-Pin With Steel Plate, Buildings", Journal Of Structural and Construction Engineering (Transaction of AIJ), Vol.86, No.788, pp.1430-1439, 2021.10 (in Japanese) https://doi.org/10.3130/ajis.86.1430

[6] SNAP Ver.7. *Finite Element Structural Analysis Software.* KOZO SYSTEM. https://www.kozo.co.jp/program/kozo/snap/index.html

[7] Richard Yip Je Too and Isoda, H. 2023. "Seismic Performance of CLT Shear Wall Infilled Hybrid Steel Frames with Concealed Steel Plates and Drift Pin Connections." J. Struct. Eng., DOI: 10.1061/JSENDH/STENG-12074

[8] Meng, L., Ohi, K. and Takanashi, K. 1992. "A simplified model of steel structural members with strength deterioration used for earthquake response analysis." *J. Struct. Constr. Eng.*, 437, 115-124. [in Japanese]. https://doi.org/10.3130/ajisx.437.0_115

[9] Matsunaga, Y., Soda, I. and Miyazu, Y. 2008. "Modeling of restoring force characteristics of wooden structures and its application to dynamic analyses," Proceeding of the 78th Architectural Research Meetings, 2007, Architectural Institute of Japan, Kanto Chapter, pp.201-204. [in Japanese]